Protein Interactions of the Porcine Circovirus Viral Protein 3

A Major Qualifying Project

Submitted to the Faculty
of the
WORCESTER POLYTECHNIC INSTITUTE

In Partial Fulfillment of the Requirements for the
Degree of Bachelor Science

By:

_____
Alec Morrison

_____
Diego Prentice

Date: April 25, 2012

Approved:

_____

Dr. Destin Heilman, Primary Advisor

Table of Contents

Acknowledgements

We would like to thank Professor Heilman for his constructive and timely feedback - without which this project would have turned out very differently. In addition to this we would like to acknowledge our lab group for being great team members and understanding the advantages of collaborative efforts in and out of the lab.

Abstract

At least half of all human cancers have mutations within the p53 gene. The chicken anemia virus viral protein 3 (CAV Apoptin) has been shown to selectively induce p53 independent apoptosis, making it a potential candidate for tumor therapy. The porcine circovirus type 2 viral protein 3 (PCV2 VP3) has also been speculated to induce apoptosis as a mechanism for viral dissemination, but the mechanisms behind such claims are poorly characterized. Homology between PCV2 VP3 and CAV Apoptin suggests that these mechanisms may be analogous in both viruses. The present study is aimed at elucidating PCV2 VP3's ability to multimerize and associate with the anaphase promoting complex/cylcosome's subunit 1 in a manner similar to CAV Apoptin. A novel FRET technique involving GFP and DsRed fluorophores bound to Apoptin was found to be successful in demonstrating protein-protein multimerization and provides a novel technique for exploring PCV2 VP3's multimeric capability. In addition to this, FLAG-tagged PCV2 VP3 constructs of both 2A and 2B isoforms were created for immunoprecipitation analysis to determine their multimeric ability and association with the APC/C subunit 1. Understanding such mechanisms may have implications in PCV2 VP3's candidacy as a novel cancer therapeutic.

Introduction

Current Cancer Treatment Strategies

Methods for treating transformed cells have experienced quite the evolution in the past few decades with current clinical practices falling into three broad categories: surgery, radiation therapy and chemotherapy. Cancer management is decided on a case-to-case basis and depends greatly on various factors such as the cancer's type and location, the degree of metastasis and the overall state of the patient. Some chemotherapy drugs have focused on exploiting one of cancer's hallmark features, uncontrollable cell division, in the hopes of slowing its growth to make tumor removal a viable option. Unfortunately, physicians have found that by targeting cells that are undergoing mitosis, normal tissue can also be severely affected. For this reason, many chemotherapeutic agents are considered to be cytotoxic (Hirsch, 2006). Additionally, when newer cancer generations develop within a patient eliciting increased mutations in the cell machinery, this form of therapy becomes increasingly less effective at targeting transformed cells.

Consequently, cancer treatment has shifted toward targeting molecular features that are unique to transformed cells in efforts to decrease the risk of damaging normal tissue. Options for treatment may include blocking certain enzymes that are important for signaling pathways such as tyrosine kinases, preventing angiogenesis through the inhibition of growth factors, or by inducing apoptosis. Many of these newer pharmaceuticals have been driven towards modulating the human tumor suppressor protein 53 (p53) which has been found to have many roles in normal cells, including activating DNA repair and preventing cell division (Harris, 1996). Specifically, it has become a popular genomic target because of the protein's natural role of

transcribing certain genes to activate signaling cascades that result in apoptosis in response to cellular stress (DNA damage or oncogene activation) (Chene, 2003).

Chemotherapeutic targeting of p53 in cancerous cells has been shown to prevent damaged tumorogenic cells with defective genomes from proliferating and spreading their mutations onto future generations, as well as reducing tumor size. p53's activity may be upregulated by inhibiting MDM2, a negative regulator of p53 that stimulates its nuclear export for degradation, which results in an increase in active p53 in the nucleus. A number of molecules have successfully achieved this including several low size peptides that are structurally similar to p53 as well as compounds such as Chlorofusin (Chene, 2003). In addition, many other chemotherapeutic drugs exploit cells' natural machinery by directly damaging cell DNA so that p53-mediated apoptosis occurs (Muller , et al., 1998). Although inducing apoptosis via p53 has shown to be successful, it is speculated that at least half of all human cancers have mutations within the p53 gene and in some cases, those who retain wild-type p53 still do not have the ability to respond to the protein correctly (Ryan, Phillips, & Vousden, 2001). Therefore, it would be advantageous to explore other therapies that do not rely on p53 to induce a cell's death program.

There are many options available to researchers when attempting to trigger apoptosis in transformed cells, but the natural signaling cascades responsible for this fall into two categories. The first is known as the extrinsic pathway which begins with the interaction of tumor necrosis factor (TNF) receptors on the cell surface and their ligands. One type of TNF is Fas (also known as CD 95 or Apo-1) which is activated when bound to its ligand, FasL, found on another cell. The protein FADD (Fas Associated Death Domain) then binds onto the cytoplasmic domain of Fas consequently recruiting two procaspase-8 molecules to form the Death Inducing Signaling

Complex (DISK). The two procaspase-8 proteins subsequently cleave and activate each other turning them into caspase-8 which can activate downstream targets procaspases-3 and 7 resulting in apoptosis. The other program for apoptosis is known as the intrinsic pathway in which proapoptotic signal-transducing molecules such Bcl-2 are activated by factors including p53. These proteins disturb and reduce the permeability of the outer-mitochondrial membrane causing cytochrome *c* (cyt c) to exit the mitochondria. Once in the cytoplasm, cyt c will bind to Apaf-1 and procaspase-9 to create the apoptosome complex which can cleave and activate procaspase-3 and 7 (Wajant, 2003).

Viruses and Apoptosis

Programmed cell death is essential in development and homeostasis in multi-cellular organisms and is the characteristic missing component of cancerous cells. Since viruses are dependent upon the exploitation of their host cell machinery for survival, their ability to affect the apoptotic process within a cell has recently been the subject of much research (Kannourakis, 2002). In some cases, it is advantageous for a virus to block or delay apoptosis until sufficient progeny have been produced as these parasites are often greatly harmed by the natural apoptotic action elicited by the host (Roulston, Marcellus, & Branton, 1999). Although a virus may benefit from avoiding the apoptotic process, the onset of programmed cell death can, in some cases, be equally advantageous. A growing number of viruses are now known to induce apoptosis purposefully at late stages of infection (Teodoro & Branton, 1997). In the final steps of apoptosis the cell becomes vacuolized as cell components, including viral particles, are encased in membrane-bound apoptotic bodies which are then absorbed into neighboring cells rather than being released into the interstitial fluid. This process of viral dissemination may represent a final and important step in the spread of progeny to neighboring cells while also evading host immune

inflammatory responses and protecting progeny virus from host enzymes and antibodies (Teodoro & Branton, 1997).

Circoviruses

It has been speculated that certain members of the *Circovirus* genus in the *Circoviridae* family induce apoptosis in an effort to disseminate and exert their pathogenic effect (Noteborn, et al., 1994). Circoviruses are small, non-enveloped, icosahedral viruses that are unique among animal viruses in having circular, single-stranded DNA genomes. Their genomes are also the smallest possessed by animal viruses (Todd, 2000). Within the circovirus family genotype, a conserved set of open reading frames contributes to their apoptotic ability. The two open reading frames, ORF1 and ORF2, border the intergenic regions of their genomes known to contain the origins of replication. ORF1 is located on the positive strand and encodes the 35.7 kDa rep protein involved in replication initiation. ORF2, called the *cap* gene, is located on the negative strand of the replicating double stranded DNA and encodes the 27.8 kDa major immunogenic capsid protein (Faurez, Dory, Grasland, & Jestin, 2009). In addition to cap and rep, a third viral protein (VP3) encoded by a third open reading frame (ORF3) exists. Although the protein encoded by ORF3 is not essential for viral replication in cultured cells, it plays a major role in virus-induced apoptosis and is involved in viral pathogenesis in vitro and in vivo (Liu, et al., 2007). Understanding the apoptotic function of VP3 in certain circoviruses, such as the chicken anemia virus and the porcine circovirus, has been the subject of much research for preventing the proliferation of transformed cells.

The Chicken Anemia Virus

Worldwide, infection of newly hatched chickens by the circovirus known as the chicken anemia virus (CAV) causes considerable health problems and economic losses in the poultry

industry (Jeurissen, Wagenaar, Pol, van der EB, & Noteborn, 1992). CAV, a small virus with a circular single-stranded DNA genome of 2.3 kb, has been shown to cause severe anemia in young chickens due to the destruction of erythroblastoid cells and cortical thymocytes which compromises their immune systems (Noteborn, et al., 1994). Thymocyte depletion can be attributed to CAV's ability to induce apoptosis in affected thymocytes as shown both *in vivo* and *in* vitro (Jeurissen, Wagenaar, Pol, van der EB, & Noteborn, 1992).

The precise mechanism by which the CAV-derived protein Apoptin induces apoptosis has been the subject of much research. Previous studies have examined whether Apoptin requires p53 activation for induction of apoptosis (Zhuang, Shvarts, Ormondt, Jochemsen, van der Eb, & Noteborn, 1995). Proteomic expression assays for Apoptin on human osteosarcoma cell lines negative for p53 have shown that Apoptin induces p53 independent apoptosis, making it a potential candidate for tumor therapy. Additionally, CAV Apoptin has also been shown to induce apoptosis in tumorigenic human fibroblasts and keratinocytes but not in normal cells (Danen-Van Oorschot, et al., 1997). This contrasts with cytotoxic drugs and radiation which preferentially kill proliferating cells in culture, irrespective of whether they are normal or transformed (Danen-Van Oorschot, et al., 1997). Apoptin's *in vitro* characteristics may preclude low *in vivo* toxicity during treatment.

In an effort to better understand the mechanism used by CAV to incite apoptosis, Noteborn et al. (Noteborn, et al., 1994) implemented immunoassays and DNA analysis to first establish that the putative open reading frame ORF3 encoding for VP3 of the CAV genome was indeed expressed in CAV-infected cells, and that, after infection, VP3 was bound to nuclear aggregates known to be apoptotic bodies. Following this study, the CAV genome has been shown to incorporate three overlapping open reading frames (ORFs) which code for three viral

proteins designated VP1, VP2, and VP3, all of which are expressed in CAV infected cells (Adair, 2000). Evidence indicates that the largest ORF, ORF1, encodes the 50 kDa VP1 capsid protein, and that ORF2 and ORF3 encode the 30 kDa VP2 scaffold protein and the 16 kDa VP3 protein, respectively (Todd, 2000). Because of its close association with the development of apoptosis in transformed cells, the name Apoptin was suggested for the VP3 protein (Adair, 2000).

Further studies aimed at elucidating Apoptin's apoptotic mechanism have demonstrated the involvement of caspases in Apoptin's apoptotic pathway (Danen-van Oorschot, van der EB, & Noteborn, 2000). Caspase-3, an important component of the apoptotic machinery present in mammalian cells, was found to be active inside cells expressing Apoptin and undergoing apoptosis. Furthermore, the results indicated that activation of downstream, but not upstream, caspases were required for rapid Apoptin-induced apoptosis. A better understanding of the mechanism of Apoptin-induced apoptosis would be helpful in determining its potential as a possible cancer therapeutic and may also provide useful information on other viral proteins that induce apoptosis.

The Porcine Circovirus

Another virus in the *circoviridae* family, known as Porcine Circovirus (PCV), has also been speculated to induce apoptosis as a mechanism for viral dissemination in a manner similar to CAV (Liu, Chen, & Kwang, 2005). Two genotypes of PCV are known to exist. The PK15 cell-derived PCV type 1 (PCV 1) was first recognized as a contaminant of continuous pig kidney cell lines and was not thought to be pathogenic to pigs (Meehan, et al., 1998). On the other hand, multiple investigations have demonstrated that there is a clear association between the disease, "post-weaning multisystemic wasting syndrome" (PMWS) and PCV type 2 (PCV 2) (Todd,

2000). PMWS, a swine disease first discovered in Canada in 1991, primarily affects pigs between 5 and 18 weeks of age and is characterized by progressive weight loss, dyspnea, tachypnea, anemia, diarrhea, and jaundice (Liu, Chen, & Kwang, 2005).

An increase in PMWS outbreaks in 2004 prompted scientific interest in the pathogenicity of PCV 2. Sequence analyses of several infected swine samples revealed that not only was there a new distinct genotype of PCV 2 named PCV 2B, but that 2B was in fact responsible for the majority (79.5%) of PMWS cases. It still remains unclear why PCV 2B has emerged as the predominant species resulting in PMWS as both PCV 2A and PCV 2B strands have been found to have no significant difference in their pathogenicity (Opriessnig, McKeown, Zhou, Meng, & Halbur, 2006). However, sequence analysis of the two strains has shown that the two are extremely similar at the nucleotide level with 98% homology (Gagnon, Tremblay, Tijssen, Venne, Houde, & Elahi, 2007). Differences between PCV-2a and PCV-2b occur within the ORF3 region, where 6 different nucleotide changes at positions 121, 207, 283, 291, 304 and 310 result in changes to the primary amino acid structure of VP3 at residues 41 (Glycine to Serine), 102 (Phenylalanine to Leucine) and 104 (Lysine to Glutamine) (see Figure 1).

Functional analysis of PCV VP3 has shown that both 2a and 2b isoforms each contain a putative Nuclear Localization Signal (NLS) and a Nuclear Export Signal (NES) which are responsible for shuttling the protein in and out of the nucleus. The NES (residues 1-64) and NLS (residues 63 to 104) for VP3 (see Figure 1) have been predicted based on Apoptin's highly characterized NES and NLS because of similarities in their apoptotic ability in transformed cells. Initially it was hypothesized that Apoptin's NLS (residues 70-121) was responsible for its tumor selectivity but it was shown that constitutive DNA damage response activation is responsible for its localization (Kucharski, Gamache, Gjoerup, & Teodoro, 2011). It has been shown

experimentally that these motifs are functional for VP3 2A, but their validity for VP3 2B has not been tested (DiLullo & Patel, 2009). The Glycine to Serine (2A to 2B) change at position 41 in VP3 is within the protein's NES and may be the cause of 2A and 2B's unequal distribution in infected pigs.

Despite the fact that PCV ORF3 may not be necessary for viral replication, VP3 has been shown to play a crucial role in infecting and causing apoptosis in porcine cells. Further investigations have also discovered that VP3 alone can trigger apoptosis in porcine cells (PK15 and Cos-7) by binding to pPirh2, an ER ubiquitin ligase which binds and ubiquinates p53 to stimulate its degradation. Once bound, the VP3-pPirh2 complex allows p53 to accumulate in the nucleus to signal the intrinsic pathway; a mechanism similar to that of designed chemotherapeutics (Liu, et al., 2007). Furthermore, recent research has added that p53 can additionally be activated by VP3 by phosphorylating JNK (Jun NH_2-terminal kinase), a protein that binds and ubiquinates p53, so that it can release it. VP3 was also found to phosphorylate p38 MAPK, a protein known to phosphorylate p53 (Wei, Zhu, Wang, & Liu, 2009). On the other hand, p53 independent pathways can also be stimulated in PK15 cells as VP3 has been shown to cleave and activate procaspase-8 to initiate the extrinsic apoptosis pathway (Liu, Chen, & Kwang, 2005). Recent experimentations in the Heilman laboratory have discovered that VP3 2B can induce apoptosis in H1299 human lung carcinoma cells (a p53 negative cell line) by signaling caspases 3 and 7 similar to that seen with Apoptin infection (Baker & Gammal, 2010). Investigating the method by which VP3 2B induces apoptosis in human cancer cells upstream of caspases 3 and 7 could be highly informative in understanding its underlying mechanisms.

CAV Apoptin and PCV2 VP3's Mechanism of Action

Although some research suggests that PCV2 VP3 may induce apoptosis in transformed cells in a p53-independent manner, the mechanisms behind such claims have yet to be discovered. Homology between PCV2 VP3 and CAV Apoptin suggests that these mechanisms, although currently undefined, may be analogous in both viruses. Therefore, results from studies aimed at elucidating CAV Apoptin's molecular mechanism for p53-independent apoptosis may shed light on PCV2 VP3's mechanistic enigma. Results from a 2004 study suggest that Apoptin expression in transformed cells induces p53-independent apoptosis via G2/M cell-cycle arrest by inhibition of APC/C function (Teodoro, Heilman, Parker, & Green, 2004). In addition to this, a 2006 study found that Apoptin must first multimerize in order to shuttle into the cell nucleus, and does so by binding onto multimerization domains that overlap the Crm-1 dependent NES, before it can initiate apoptosis (Heilman, Teodoro, & Green, 2006). The ability of PCV2 VP3 to multimerize and to induce p53-independent apoptosis in transformed cells via association with sub-unit 1 of the APC/C has yet to be determined. The capacity of PCV2 VP3 to multimerize and induce of G2/M cell-cycle arrest could advance our understanding and current knowledge of the virus apoptotic pathway.

To assess the capability of PCV2 VP3 to multimerize in a manner similar to its CAV Apoptin homolog, a novel fluorescence resonance energy transfer (FRET) technique involving GFP and DsRed tagged proteins will be used to detect protein-protein interactions of VP3. Following transfection of Flag-tagged VP3 constructs into a p53-negative non-small cell lung carcinoma cell line, immunoprecipitation analysis of the VP3 constructs and their interaction with APC sub-unit 1 should allow for accurate determination of PCV2 VP3's association with the APC/C cyclosome, as well as its ability to induce G2/M cell-cycle arrest in transformed cells.

Understanding the possible mechanisms by which VP3 can initiate tumor-selective apoptosis may have implications for VP3's candidacy as a cancer therapeutic in patients with p53 mutations.

Materials and Methods

Midiprep of PCV-2a/b in GFP Vectors and Apoptin in GFP and DsRed Vectors

PCV-2a and 2b VP3 in GFP Vector stock solutions and Apoptin in GFP and DsRed Vector stock solutions were transformed into chemically competent *E. coli*. This was achieved by first adding 1µL of each stock DNA to 70 µL of DH5α *E. coli* cells. After a 15 min incubation on ice to allow DNA complex formation, the cells were heat shocked in a 42°C water bath for 60 sec and then returned to ice for 2 min. Following this, 450 µL of LB recovery media was added to each tube and the *coli* were incubated for 1 hour at 37°C on a rotator. After the incubation period, 20 µL of the cells were added to 50 mL of LB Broth with 50 µL of 1000x kanamycin and cultured overnight at 37°C in a shaker. Once cultured, the cells were pelleted at 5,000 x *g* for 10 minutes. Following this, plasmid DNA was purified using Promega's PureYield Plasmid Midiprep system (Cat. No. A2492).

A 0.9% agarose gel electrophoresis was run in order to verify the integrity of our plasmid DNA preparations. This was achieved by creating an agarose gel using 1X Tris-Acetate-EDTA (1M Acetate and 0.05M EDTA) and 5 µL of ethidium bromide for staining. Plasmid DNA was prepared for electrophoresis by mixing 5 µL of ddH_2O, 2 µL of 5X DNA Loading Dye (30% glycerol, 0.25% bromophenol blue, 69.75% ddH_2O), and 3 µL of plasmid DNA. Once the gel had dried, 10 µL of each prepared DNA was loaded into the gel along with 10 µL of a 2-log DNA ladder. The gel was covered with 1X TAE buffer and run at 90V for 45 min before being imaged under a UV lamp.

Cloning into FLAG Vector

In order to insert PCV 2a and 2b VP3 DNA into a 3xFLAG Vector (Sigma), the target DNA had to be first restricted out of the pEGFP Vector. BamHI and EcoRI restriction enzymes

were used to restriction PCV 2a and 2b VP3 DNA out of their pEGFP Vectors. The digests were set up by combining 2 µL of Buffer E, 3 µL of plasmid DNA, 9 µL of H_2O, 3 µL of EcoRI, and 3 µL of Bam HI into a single eppendorf tube. The mixtures were incubated for 3 hours in a 37°C water bath before being run on a 0.9% agarose gel as previously described. The gel was imaged over a UV lamp to confirm the presence of insert DNA.

Following electrophoresis, the DNA bands corresponding to 2a and 2b VP3 DNA were purified from the gel using Promega's Wizard SV Gel and PCR Clean-up System. DNA bands were excised from the gel and placed in a pre-weighed eppendorf tube. Once the weight of the gel slice was determined, 10 µL of Membrane Binding Solution was added per 10 mg of gel slice prior to being vortexed and incubated at 60°C until the gels dissolved. The gel mixtures were transferred to a Minicolumn assembly and centrifuged at 16,000 x *g* for 1 min. After discarding the flowthrough, the minicolumns were re-inserted into collection tubes and 700 µL of Membrane Wash Solution was pulled through the minicolumns by centrifugation at 16,000 x *g* for 1 min. The process was then repeated with 500 µL of Membrane Wash Solution and a 5 min centrifugation at 16,000 x *g*. The flowthrough was discarded and the column assembly was re-centrifuged with the lid open to remove any residual ethanol. After this, the Minicolumn was transferred to an eppendorf tube and 50 µL of Nuclease-Free water was pulled through the minicolumns by centrifugation at 16,000 x *g* for 1 min.

T4 DNA ligase was used to clone the purified PCV-2a and 2b VP3 DNA into the 3xFLAG Vector. The ligations were set up on ice by combining 2 µL of FLAG Vector, 6 µL of 2a/2b DNA, 1 µL T4 DNA Ligase, 2 µL Ligase Buffer, and 9 µL of H_2O into one eppendorf. A control was also made by replacing 6 µL of 2a/2b DNA with 6 µL of H_2O. Following an

overnight incubation at 4°C, the DNA was transformed into DH5α chemically competent *E. coli* cells as previously described and then plated on LB-Amp plates.

DNA Uptake Screening

Random colonies from the LB-Amp plates of 2a and 2b transformed DNA were screened to determine which one had successfully uptook 2a/2b VP3 DNA inserted into the 3xFLAG Vector. This was accomplished by culturing 5 separate colonies from each plate in 2 mL of LB broth and 2 μL of 1000x Ampicillin overnight with shaking. A small scale plasmid DNA preparation was performed on 1.5 mL of each culture and the remaining 0.5 mL was stored at 4°C. Each 1.5 mL culture was centrifuged at 12,000 x *g* for 30 seconds at 4°C and the supernatant was discarded. The bacterial pellets were re-suspended in 100 μL of ice-cold MPS I solution (50 mM glucose, 25 mM Tris-Cl pH 8.0, 10 mM EDTA pH 8.0) by rigorous vortexing. Once re-suspended, 200 μL of MPS II solution (0.2 N NaOH, 1% SDS) was added and mixed by inverting 5 times, followed by 150 μL of ice-cold MPS III solution (60 mL 5 M potassium acetate, 11.5 mL glacial acetic acid, 28.5 mL H_2O). The mixtures were vortexed upside down for 10 seconds to disperse MPS III solution through the viscous bacterial lysate and incubated on ice for 5 min. After the incubation, the suspensions were centrifuged at 12,000 x *g* for 5 min at 4°C. The supernatants were transferred to a new tube and the DNA was precipitated with 2 volumes of ethanol at room temperature for 2 minutes. Once precipitated, the mixtures were centrifuged at 12,000 x *g* for 5 minutes at 4°C and the supernatants were discarded. The process was repeated with 1 mL of 70% ethanol and the DNA was re-suspended in 50 μL of TE buffer at pH 8.0.

The 2a and 2b VP3 DNA purified from 5 separate colonies were verified via restriction digests run on a 0.9% agarose gel electrophoresis as previously described. The stored cultures from the colonies found to contain intact 2a and 2b VP3 DNA ligated into a 3xFLAG Vector

were added to 50 mL of LB Broth with 50 µL of 1000x kanamycin and cultured overnight at 37°C with shaking. Following this, plasmid DNA from each culture was purified using Promega's Midiprep Kit as previously described. The DNA purity was verified on a 0.9% agarose gel as previously described. The gel was imaged over a UV lamp to confirm the presence of insert DNA. Once verified, aliquots of the purified DNA were sent to Macrogen USA for sequencing.

Construct Transfection into H1299 Cells

H1299 human lung carcinoma cells were maintained in Dulbecco's Modified Eagle Medium (DMEM) supplemented with 10% fetal bovine serum (FBS) and 1% antibiotic formulation PSF (penicillin, streptomycin, and fungizone) at 37°C in 5% CO_2 air. Cells analyzed by fluorescence microscopy were grown in 6-well plates containing microscope cover slips, while cells used for immunoprecipitation were grown in 100mm Falcon Tissue Culture (TC) plates. FLAG-VP3 2a/2b, GFP-VP3 2a/2b, FLAG-Apoptin, GFP-Apoptin, DsRed-Apoptin, and 3xFLAG vector constructs were all transfected into H1299 cells that were ~80% confluent using a Qiagen Effectene Transfection Kit (Cat. No. 301425).

For fluorescence microscopy, DNA was diluted with EC buffer to a final concentration of 0.064 µg/µL for GFP-Apoptin and 0.128 µg/µL for DsRed-Apoptin. Once diluted, 6.4 µL of enhancer was added and the mixture was vortexed. After a 2 min incubation, 20 µL of effectene reagent was added and complexes were allowed to form for 15 min at room temperature. During complex formation, growth media was aspirated from the wells and cells were washed with 1x Phosphate Buffered Saline (PBS) before being resuspended in 1.6 mL of fresh media. Following the 15 minute incubation, DNA complexes were mixed with 1.2 mL of media before ~700 µL was added dropwise to each of 2 wells.

Cell transfections for immunoprecipitation experiments were prepared in the same manner except 60 µL of effectene reagent was used and complexes were resuspended in 3 mL of media to give a final volume of 10 mL of growth media in the TC plates.

Fluorescence Microscopy

Infected cells were incubated for 24 hours before the growth media was aspirated and washed with 1x PBS. The cells on the cover slips were fixed in 4% paraformaldehyde (diluted in 1x PBS) before being mounted onto slides using 20 µL of mounting media (1x PBS with 2.5% DABCO and 50% glycerol). The slides were sealed with nail polish and allowed to air dry in the dark. Cells were observed on a Leica SP5 Confocal Microscope and the FRET Sensitized Emission (SE) wizard on the Leica Application Suite was used to calculate FRET efficiencies.

FRET analysis using the confocal microscope began by imaging uncombined GFP and DsRed-Apoptin transfected cells to give correction constants for eliminating the excitation and emission cross talk. An Argon and 561nm laser was used to excite GFP-Apoptin and DsRed-Apoptin constructs respectively at their peak intensities of 488 nm and 557 nm, respectively (see Figure 6d). Once fluorescence intensities, PMT gain and laser dose factors were calibrated for ideal donor (GFP) and acceptor (DsRed) controls, correction images were taken and the settings were saved into the program. The FRET sample (containing both donor and acceptor proteins) was imaged and excited at 488 nm. In each cell viewed, 6 regions of interest (ROI) were selected for precise calculation of FRET efficiencies ($E_A(i)$) using the following formula:

$$E_A(i) = \frac{(B - A) \times (b - C) \times c}{C}$$

Where A = Donor emission; B = FRET emission; b = Donor emission + crosstalk ratio; C = Acceptor emission; c = Accepter emission + crosstalk ratio based on methods described previously (Wouters, Verveer, & Bastiaens, 2001).

Immunoprecipitation and Western Blotting

For multimerization experiments, H1299 cells were co-transfected with either PCV VP3 2A in GFP and FLAG Vectors, or PCV VP3 2B in GFP and FLAG Vectors. As a positive control, H1299 cells were co-transfected with CAV Apoptin in GFP and FLAG Vectors, while pEGFP-C1 DNA was used as a negative control. For VP3-CDC 27 interaction experiments, FLAG-VP3 2A and 2B construct DNA were transfected as indicated above. Following a 24 hour incubation period, growth media was aspirated and the TC plates were washed 5 times in 1x PBS. After the final wash, ~1 mL of 1x PBS was left behind and the cells were scraped and dispersed in the leftover PBS before being transferred to pre-chilled eppendorf tubes. Cells were lysed by centrifugation at 10,000 x *g* for 5 min and the supernatant was discarded. Cell pellets were then resuspended in 500 µL of Buffer X (50 mM Tris [pH 8.5], 250 mM NaCl, 1 mM EDTA and 1% NP-40) supplemented with 100 µL of protease inhibitor and left on ice for 20 min. After the incubation, cell debris was pelleted by centrifugation at 10,000 x *g* for 5 min and the supernatants were transferred to a new pre-chilled eppendorf tubes. These solutions were then incubated with 25 µL of EZview Red α-Flag M2 affinity beads (Sigma) at 4°C for 4 hours on a rotator. After 4 hours the beads were washed 5 times in 500 µL of Buffer X by pulse centrifugation and bound protein was resuspended in 100 µL 1x Protein Loading Buffer (0.5M Tris-HCL [pH 6.8], 10% SDS (w/v), 5% β-mercaptothenol (v/v), 30% glycerol (v/v) & 0.02% bromophenol blue) and eluted by boiling on a 95°C heat block for 5 min.

Protein samples were separated by SDS-polyacrylamide gel electrophoresis using a 16% polyacrylamide resolving gel. Once the gel had dried, 30 µL of each sample was loaded into the gel and it was run for ~2 hrs at a constant current of 35 mAmps. The gels were then transferred to nitrocellulose paper by assembling a transfer sandwich and running them at a constant current of 200 mAmps for 1 hour. Blots were then blocked with 5% milk blocking buffer overnight at 4°C on an agitator. The next day the blots were washed 5 times on an agitator for 5 min at room temperature with Tris-Buffered Saline with 0.5% Tween-20 solution (TBS-T) and then probed with either primary α-Flag M2 MAb (Sigma), α-GFP MAb (Clontech) or α-APC1 antibody diluted (1/5,000) in TBS-T for 1 hr on an agitator before being washed 5 times in TBS-T. After the wash, all blots were probed with secondary Donkey α-rabbit antibody diluted (1/20,000) in TBS-T for 1 hr on an agitator. Blots were washed an additional 5 times in TBS-T and twice in TBS. Membranes were then developed using Promega's HRP chemiluminescence ECL reagents and allowed to incubate for 5 min in complete darkness and were imaged.

Results

Formation and Verification of DNA Constructs

To increase the initial amount of PCV 2A and 2B VP3 in GFP Vector stock solutions and Apoptin in GFP and DsRed Vector stock solutions, plasmid DNA were first transformed into chemically competent *E. coli* cells and allowed to replicate *in vivo*. From there, the plasmid DNA constructs were isolated from the bacterial cells using large scale plasmid DNA purification and a restriction digest was performed on the DNA using the restriction enzymes BamHI and EcoRI. The presence of inserts and the integrity of the Vector DNA were verified using a 0.9% agarose gel electrophoresis of the restriction digest.

Figure 3 and Figure 4A show the presence of Apoptin in GFP and DsRed Vectors along with the presence of 2A and 2B VP3 DNA in GFP Vectors, respectively. In both Figure 1 and Figure 4A the band pattern of the cut plasmids near 0.3 kb - coupled with the GFP and DsRed Vector bands near 4.7 kb - indicates that both Apoptin and VP3 DNA are intact within their respective vectors. This data confirms the successful large-scale preparation of purified plasmid DNA. Once confirmed, a UV-Vis spectrometer was used to determine the concentration of DNA in each purification. The concentrations of 2A and 2B VP3 in pEGFP-C1 vector were found to be 0.73 μg/μL, and 2.23 μg/μL, respectively. Apoptin in pEGFP-C1 and pDsRed1-N1 Vectors were determined to be 0.31 μg/μL and 3.01 μg/μL, respectively.

PCV 2A and 2B VP3 was cloned into a 3xFLAG Vector which contains a 23 amino-acid long epitope found to be effective for immunoprecipitation and western blotting. To insert PCV 2A and 2B VP3 DNA into a 3xFLAG Vector, the target DNA had to be first restricted out of the GFP Vector it was in. This was done by using BamHI and EcoRI restriction enzymes in restriction digests of PCV 2A and 2B VP3 DNA in GFP Vector. A 0.9% agarose gel

electrophoresis was used to assess the ability of BamHI and EcoRI to excise 2A and 2B VP3 DNA. Figure 4A depicts the gel resulting from the double digest of 2A and 2B DNA out of the GFP Vector. The dropout inserts around 0.3 kb correspond to 2A and 2B VP3 DNA and the larger bands around 4.7 kb represent linearized GFP Vector. The clear, precise bands in Figure 4A demonstrate that 2A and 2B VP3 DNA was correctly excised from the GFP Vector.

In order to obtain purified 2A and 2B VP3 DNA to ligate into a 3xFLAG Vector, insert bands containing 2A and 2B VP3 DNA were extracted from the gel of the GFP Vector restriction digest. The purified DNA was then ligated into the 3xFLAG Vector using a T4 DNA Ligase enzyme. To increase the quantity of 3xFLAG Vector constructs and verify their integrity, chemically competent *E. coli* were transformed with ligated DNA and allowed to replicate in *vivo*. In order to screen for screen for the *coli* which expressed intact ligations of 2A and 2B VP3 DNA in a 3xFLAG Vector, the transformations were plated on LB-AMP plates and 5 colonies from each plate were chosen at random to be cultured under conditions containing 1000X Ampicillin. Colonies demonstrating bacterial resistance to Ampicillin allowed for an initial screening for the successful uptake of the exogenous 2A and 2B VP3 DNA ligated into a 3xFLAG vector. To verify that 2A and 2B VP3 DNA was correctly ligated into the 3xFLAG vector, the plasmid DNA from colonies which passed the initial screen was purified and restricted using BamHI and EcoRI restriction enzymes.

Figure 5 depicts a 0.9% agarose gel electrophoresis of the restriction digests of both 2A and 2B ligations. Successful uptake of ligated DNA was seen in three out of five 2A VP3 colonies and in two out of five 2B VP3 colonies. The band pattern of the cut plasmids in Figure 4B and Figure 5 suggest that both 2A and 2B VP3 DNA were successfully cloned into a

3xFLAG vector, as seen from the characteristic dropout 2A and 2B VP3 inserts around 0.3 kb and the linearized Vector DNA at 6.7 kb.

To obtain purified construct DNA, the leftover cultures from the colonies confirmed to contain the FLAG Vector constructs were Midiprepped. Purified plasmid DNA was further verified using a 0.9% agarose gel electrophoresis of a restriction digest containing BamHI and EcoRI restriction enzymes. Figure 4B shows the gel of the restriction digest of the plasmid purifications containing characteristic band sizes for 3xFLAG and 2A/B VP3 DNA. Sequence analysis of the constructs using CLC Sequence Viewer 6 further confirmed that the correct amino acid sequences for the 3xFLAG epitope and VP3 were present in the constructs (Figure 2).

A UV-Vis spectrometer was used to determine the concentration of DNA in each purification. The concentrations of 2A and 2B VP3 in 3xFLAG vector were found to be 1.0682 μg/μL and 0.5112 μg/μL, respectively.

FRET between GFP and DsRed Tagged Apoptin Constructs

To determine whether the GFP and DsRed tagged Apoptin constructs could multimerize and FRET with each other *in vivo,* 6.4 μg of GFP-Apoptin and 12.8 μg of DsRed-Apoptin construct DNA was combined in 200 μL of EC buffer and transfected into H1299 cells and incubated at 37°C. Cells were additionally transfected with GFP and DsRed-Apoptin alone as controls. After 24 hours, cells were mounted onto microscope slides and imaged using fluorescence microscopy. The FRET Sensitized Emission (SE) wizard on the Leica Application Suite was used to calculate FRET efficiencies.

Figure 6b depicts how the efficiencies were calculated in the wizard. First, control donor GFP samples (top left panel) and acceptor DsRed samples (bottom left panel) were excited using

an Argon and 561nm laser at 488 nm and 557 nm, respectively, and emission was detected at 509 nm and 592 nm, respectively, to give correction constants for eliminating excitation and emission cross talk. The FRET sample (top right panel) was then excited at 488 nm and light emitted at 592 nm was detected using a sequential line by line scan of the entire cell. The FRET efficiency was then calculated by factoring in acceptor emission and both donor and acceptor cross talk ratios.

Six cells expressing high levels of fluorescence were selected for analysis and individual regions of interest (ROI) in each cell were chosen to evaluate FRET efficiencies. Figure 6a shows the average FRET efficiencies from 6 ROIs generated for each cell giving an overall efficiency of 32.86%. The size of the regions of interest did not affect the resulting FRET efficiency as there was no significant difference between efficiencies calculated using either a small or large ROI (Figure 6a).

Discussion

The ability of viral proteins to selectively induce cell death in cancerous cells has become a very broad and important field of research for cancer therapy. Results from studies on the third viral protein of the chicken anemia virus (Apoptin) have emphasized its importance as a novel therapy for cancers lacking the p53 tumor suppressor protein. For this reason, the mechanism by which Apoptin initiates programmed cell death specifically in transformed cells has been the subject of much research. Recent studies strongly suggest that the protein multimerizes in the nuclei of transformed cells before associating with the APC/C to inactivate MDC1 and prevent DNA damage foci from forming, which results in apoptosis (Kucharski, Gamache, Gjoerup, & Teodoro, 2011). In this report we extend these findings to the less characterized, but highly homologous third viral protein of the porcine circovirus type 2 (PCV 2 VP3). We demonstrate that the homology between Apoptin and VP3 allows for analogous investigations into their mechanism of action. By using Apoptin's well-defined ability to multimerize as a positive control for multimeric studies on PCV 2 VP3 2A/B, we were able to show that not only do GFP and DsRed tagged Apoptin constructs undergo fluorescence resonance energy transfer, but also that GFP and DsRed concatemers provide a novel method for investigating *in vivo* protein-protein interactions of viral proteins.

Although fluorescence resonance energy transfer (FRET) provides strong evidence of protein associations within the natural environment of the living cell, standalone FRET measurements are considered by some to be insufficient evidence for proving direct physical protein interactions (Periasamy & Day, 2005). For this reason, we designed and synthesized DNA constructs to be used in immunprecipitation experiments involving VP3 2A and 2B in FLAG and GFP vectors to provide more information about their ability to multimerize. We were

able to create and purify FLAG-tagged PCV 2 VP3 constructs for both 2A and 2B isoforms using DNA excised from a GFP vector construct. The integrity and purity of our DNA was evaluated using an agarose gel electrophoresis of our restricted construct DNA. Characteristic bands corresponding to both GFP and FLAG Vector linearized DNA coupled with plasmid cutouts of VP3 2A and 2B DNA confirmed the success of our cloning procedure. Sequence analysis of plasmid constructs further supported the results from the gel electrophoresis.

In addition to confirming proper sequence construction of our plasmids, sequence analysis of PCV 2A, 2B, and CAV Apoptin was performed to explore their level of homology. In accordance with previous studies, we were able to observe significant sequence homology between the NES and NLS residues of all three proteins. These results support our claim for using experiments performed on CAV Apoptin as models for evaluating PCV 2 VP3's mechanism of action.

Whereas previous studies have shown that DsRed supports FRET in GFP-DsRed constructs separated by a small linker chain, none have used this technique to examine a viral protein's ability to multimerize in the nucleus of transformed cells. Co-transfection of GFP and DsRed Apoptin constructs into p53 negative H1299 human lung carcinoma cells enabled us to effectively evaluate the feasibility of this FRET technique for studying viral protein-protein interactions *in vivo*. Whereas previous studies have reported average FRET efficiencies of around 25% (Erickson, Moon, & Yue, 2003), our evaluation over 36 ROIs resulted in an average of 38.67%. Comparison of small and large ROIs also revealed that there was no significant deviation in FRET efficiency between the two.

The significance of this data is three-fold. First, the result presented here that GFP and DsRed fluorophores can successfully undergo FRET is in agreement with previous studies

claiming DsRed as a potential FRET partner with GFP. Second, our results demonstrating successful FRET between GFP and DsRed tagged Apoptin localized in the nucleus directly supports previous observations that Apoptin multimerizes in the nucleus of transformed cells before exerting its pathogenic effect. The activation of FRET between multimers of GFP and DsRed tagged Apoptin provides a definitive proof of principle that this novel technique can be used as a model for assessing PCV 2 VP3's ability to multimerize in transformed cells. Finally, from a broader standpoint our reported 13% increase in FRET efficiency as compared to previously recorded data demonstrates for the first time that DsRed as a FRET partner with GFP can be employed to investigate viral protein interactions.

Successful immunoprecipitation of our VP3 2A and 2B in FLAG Vectors using FLAG antibody - coupled with a blot for VP3 2A and 2B in GFP vectors - would provide sufficient evidence to conclude that VP3 does in fact multimerize similar to its CAV Apoptin homolog. Furthermore, the success or failure of VP3's interaction with APC/C subunit 1 will enable formidable conclusions to be drawn regarding VP3's apoptotic pathway. Although immunoprecipitation experiments are ongoing, if successful, they could yet reveal PCV 2 VP3's mechanism of action and garner further support for the conclusions drawn from FRET.

Results from the present study suggest that PCV 2 VP3's capacity to initiate tumor-selective apoptosis may be better understood through its CAV Apoptin homolog. Based on the success of GFP and DsRed as FRET partners while studying Apoptin protein-protein interaction, we propose that PCV 2 VP3 2A and 2B tagged with GFP and DsRed fluorophores could provide sufficient evidence to draw conclusions on PCV 2 VP3's ability to multimerize. In addition to this, conclusions drawn from immunoprecipitation analysis of PCV VP3 2A and 2B isoforms in FLAG Vectors would solidify multimeric conclusions from FRET, and allow for investigation

into VP3's possible interaction with subunit 1 of the APC/C. The combined results from both methods could broaden our understanding of the mechanisms by which PCV 2 VP3 induces programmed cell death and may have implications for VP3's candidacy as a cancer therapeutic in patients with p53 mutations.

Bibliography

Adair, B. (2000). Immunopathogenesis of Chicken Anemia Virus Infection. *Devlopmental & Comparative Immunology*, 247-255.

Baker, K. M., & Gammal, R. S. (2010). Investigating the Ability of Porcine Circovirus 2 to Selectively Target and Kill Cancer Cells. *WPI Major Qualifying Project*.

Chene, P. (2003). Inhibiting the p53-MDM2 Interaction: An Important Target for Cancer Therapy. *Nature Reviews: Cancer*, 102-109.

Danen-Van Oorschot, A., Fischer, D., Grimbergen, J., Klein, B., Zhuang, S., Falkenburg, J., et al. (1997). Apoptin induces apoptosis in human transformed and malignant cells but not in normal cells. *The National Acadaemy of Sciences of the USA*, 5843-5847.

Danen-van Oorschot, A., van der EB, A., & Noteborn, M. (2000). The Chicken Anemia Virus-Derived Protein Apoptin Requires Activation of Caspases for Induction of Apoptosis in Human Tumor Cells. *Journal of Virology*, 7072-7078.

DiLullo, N. M., & Patel, Z. H. (2009). Functional Analysis of Porcine Circovirus 2 VP3 Localization Through Truncation Mutagenesis. *WPI Major Qualifying Project*.

Erickson, M., Moon, D., & Yue, D. (2003). DsRed as a Potential FRET Partner with CFP and GFP. *Biophysical Journal*, 599-611.

Faurez, F., Dory, D., Grasland, B., & Jestin, A. (2009). Replication of Porcine Circoviruses. *Virology Journal*, 6:60.

Gagnon, C. A., Tremblay, D., Tijssen, P., Venne, M.-H., Houde, A., & Elahi, S. M. (2007). The emergence of porcine circovirus 2b genotype (PCV-2b) in swine in Canada. *The Canadian Veterinary Journal*, 811-819.

Harris, C. C. (1996). Structure and Function of the p53 Tumor Suppressor Gene: Clues for Rational Cancer Therapeutic Strategies. *Journal of National Cancer Institute*, 1442-1455.

Heilman, D., Teodoro, J. G., & Green, M. R. (2006). Apoptin Nucleocytoplasmic Shuttling Is Required for Cell Type-Specific Localization, Apoptosis, and Recruitment of the Anaphase-Promoting Complex/Cyclosome to PML Bodies. *Journal of Virology*, 7535-7545.

Hirsch, J. (2006). An Anniversary for Cancer Chemotherapy. *The Journal of the American Medical Association*, 1518-1520.

Jeurissen, S., Wagenaar, F., Pol, J., van der EB, A., & Noteborn, M. (1992). Chicken Anemia Virus Causes Apoptosis of Thymocytes after In Vivo Infection and of Cell Lines after In Vitro Infection. *Journal of Virology*, 7383-7388.

Kannourakis, S. H. (2002). A time to kill: viral manipulation of the cell death program. *Journal of General Virology*, 1547-1564.

Kucharski, T., Gamache, I., Gjoerup, O., & Teodoro, J. (2011). DNA Damage Response Signaling Triggers Nuclear Localization of the Chicken Anemia Virus Protein Apoptin. *Journal of Virologu*, 12638-12649.

Liu, J., Chen, I., & Kwang, J. (2005). Characterization of a Previously Unidentified Viral Protein in Porcine Circovirus Type 2-Infected Cells and Its Role in Virus-Induced Apoptosis. *Journal of Virology*, 8262-8274.

Liu, J., Zhu, Y., Chen, I., Lau, J., He, F., Lau, A., et al. (2007). The ORF3 Protein of Porcine Circovirus Type 2 Interacts with Porcine Ubiquitin E3 Ligase Pirh2 and Facilitates p53 Expression in Viral Infection. *Journal of Virology*, 9560-9567.

Meehan, B., McNeilly, F., Todd, D., Kennedy, S., Jewhurst, V., Ellis, J., et al. (1998). Characterization of Novel Circovirus DNAs associated with Wasting Syndromes in Pigs. *Journal of Virology*, 2171-2179.

Muller , M., Wilder, S., Bannasch, D., Israeili, D., Lehlbach, K., Li-Weber, M., et al. (1998). p53 Activates the CD95 (APO-1/Fas) Gene in Response to DNA Damage by Anticancer Drugs. *Journal of Experimental Medicine*, 2033-2045.

Noteborn, M., Todd, D., Verschueren, A., De Gauw, H., Curran, W. L., Veldkamp, S., et al. (1994). A Single Chicken Anemia Virus Protein Induces Apoptosis. *Journal of Virology*, 346-351.

Opriessnig, T., McKeown, N. E., Zhou, E.-M., Meng, X.-J., & Halbur, P. G. (2006). Genetic and experimental comparison of porcine circovirus type 2 (PCV2) isolates from cases with and without PCV2-associated lesions provides evidence for differences in virulence. *Journal of General Virology*, 2923-2932.

Periasamy, A., & Day, R. N. (2005). *Molecular Imaging: FRET Microscopy and Spectroscopy*. Elsevier.

Roulston, A., Marcellus, R., & Branton, P. (1999). Viruses and Apoptosis. *Annual Review of Microbiology*, 577-628.

Ryan, K. M., Phillips, A., & Vousden, K. H. (2001). Regulation and Function of the p53 Tumor Suppressor Protein. *Current Opinion in Cell Biology*, 332-337.

Teodoro, J. G., Heilman, D. W., Parker, A. E., & Green, M. R. (2004). The viral protein Apoptin associates with the anaphase-promoting complex to induce G2/M arrest and apoptosis in the absense of p53. *Genes & Development*, 1952-1957.

Teodoro, J., & Branton, P. (1997). Regulation of Apoptosis by Viral Gene Products. *Journal of Virology*, 1739-1746.

Todd, D. (2000). Circoviruses: Immunosuppressive threats to avian species: A review. *Avian Pathology*, 373-394.

Wajant, H. (2003). Death Receptors. *Essays in Biochemistry*, 53-71.

Wei, L., Zhu, Z., Wang, J., & Liu, J. (2009). JNK and p38 Mitogen-Activated Protein Kinase Pathways Contribute to Porcine Circovirus Type 2 Infection. *Journal of Virology*, 6039-6047.

Wouters, F. S., Verveer, P. J., & Bastiaens, P. I. (2001). Imaging biochemistry inside cells. *TRENDS in Cell Biology*, 203-211.

Zhuang, S.-M., Shvarts, A., Ormondt, H., Jochemsen, A., van der Eb, A. J., & Noteborn, M. H. (1995). Apoptin, a Protein Derived from Chicken Anemia Virus, Induces p53-independant Apoptosis in Human Osteosarcoma Cells. *Cancer Research*, 486-489.

Figures and Tables

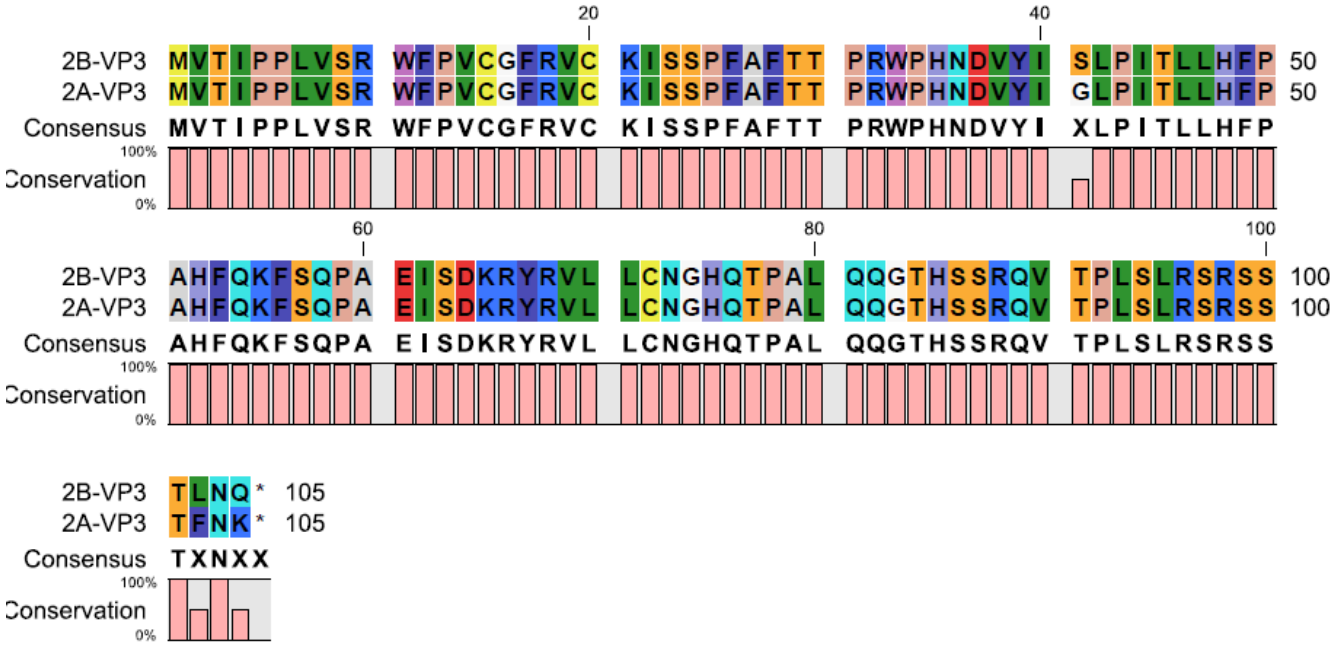

Figure 1 - Amino Acid Sequence Comparison of PCV 2A and B VP3. There are 3 key residue substitutions between the two isoforms of PCV 2: a Serine-Glycine change at position 41, a Leucine-Phenylalanine change at position 102 and a terminal Glutamine-Lysine change at position 104.

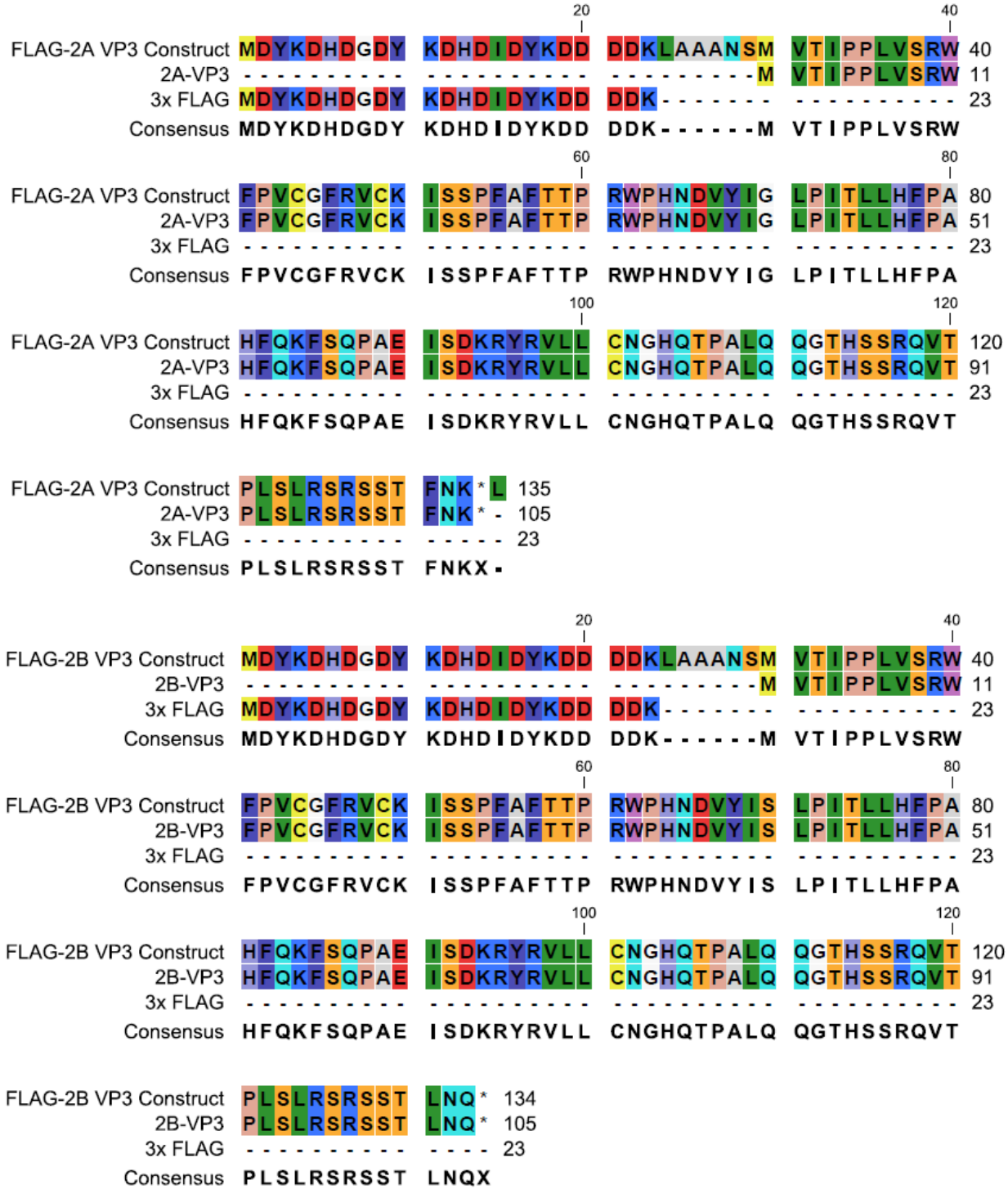

Figure 2 - Amino Acid Sequence Analysis of FLAG-2A and B VP3 Constructs. PCV 2A and B VP3 proteins were succesfully restricted from their pEGFP-C1 plasmids and ligated into 3xFLAG vectors.

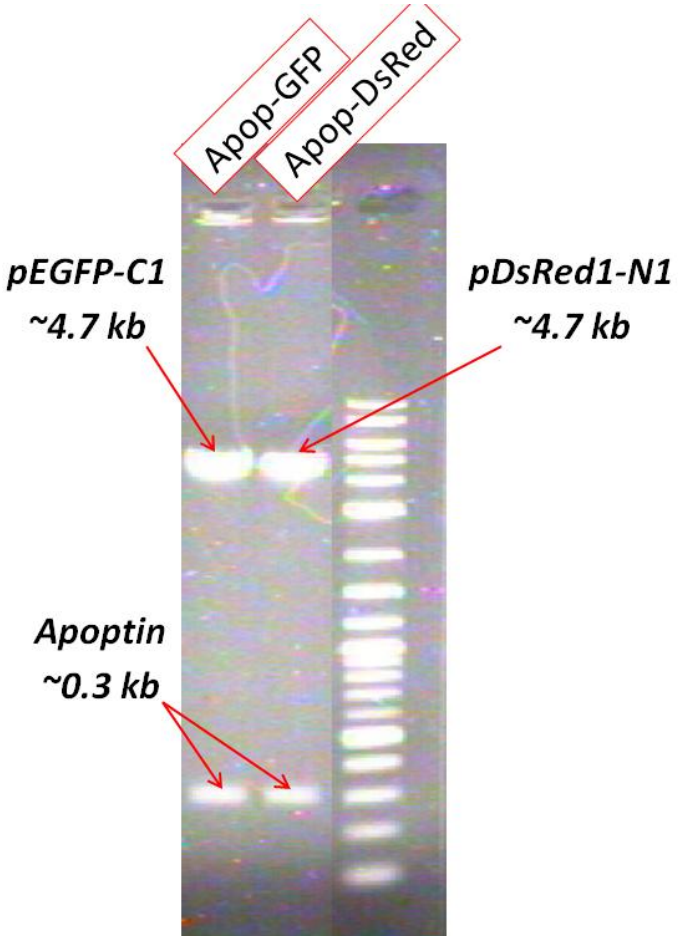

Figure 3 - Gel Electrophoresis of CAV Apoptin GFP and DsRed Construct Restriction Digests. CAV Apoptin DNA restricted out of pEGFP-C1 and pDsRed1-N1 Vectors. Bands at 4.7 kb correspond to pEGFP-C1 and pDsRed1-N1 DNA and bands at ~0.3kb correspond to restricted CAV Apoptin DNA using BamHI and EcoRI restriction enzymes.

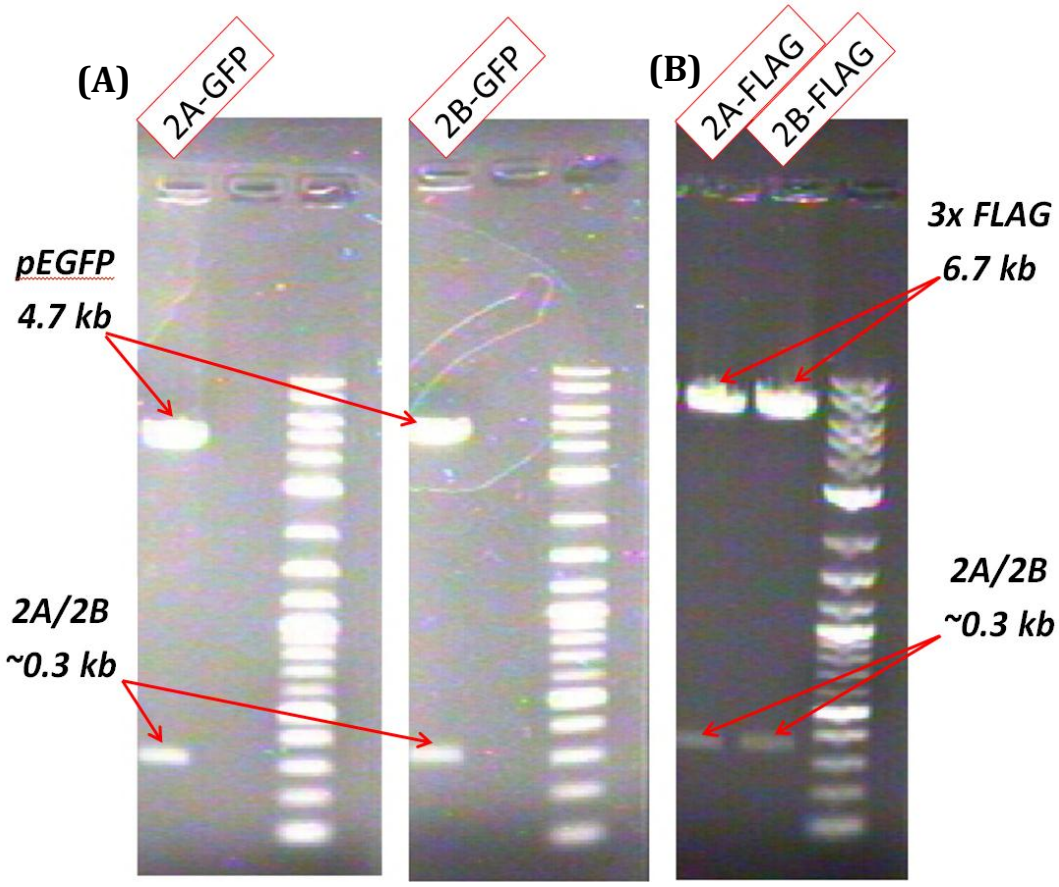

Figure 4 - Gel Electrophoresis of PCV VP3 2a/b GFP and FLAG construct restriction digests. (A) VP3 2A and 2B DNA restricted out of pEGFP vector prior to ligation into 3x FLAG. Bands at 4.7 kb correspond to pEGFP DNA and bands at ~0.3kb correspond to restricted VP3 2A and 2B DNA using BamHI and EcoRI restriction enzymes. (B) VP3 2A and 2B DNA restricted out of 3xFLAG vector to demonstrate successful construct creation. Bands at 6.7 kb correspond to 3xFLAG DNA and bands at ~0.3kb correspond to restricted VP3 2A and 2B DNA using BamHI and EcoRI restriction enzymes.

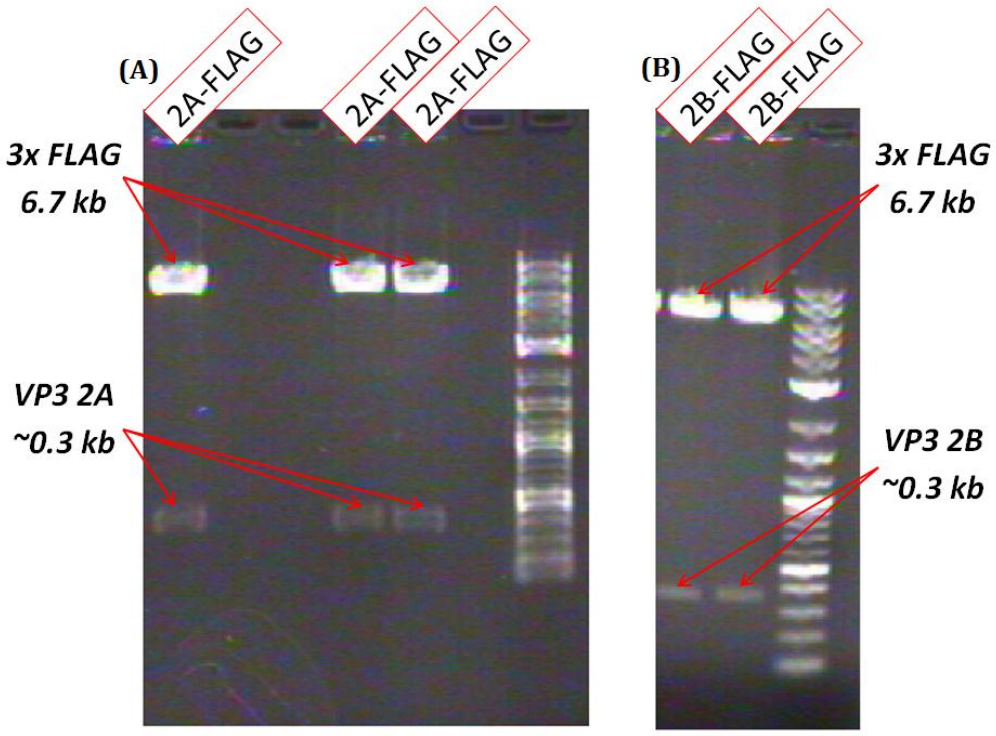

Figure 5 - Gel Electrophoresis of PCV VP3 2a/b FLAG Construct Restriction Digest for DNA Uptake Screening. (A) PCV 2a VP3 DNA restricted out of 3xFLAG Vector. Lanes containing bands at 6.7 kb and ~0.3kb correspond to colonies which uptook 3xFLAG linearized Vector DNA and restricted 2a VP3 DNA, respectively. DNA was restricted using BamHI and EcoRI restriction enzymes. (B) PCV 2b VP3 DNA restricted out of 3xFLAG Vector. Lanes containing bands at 6.7 kb and ~0.3kb correspond to colonies which uptook 3xFLAG linearized Vector DNA and restricted 2a VP3 DNA, respectively. DNA was restricted using BamHI and EcoRI restriction enzymes.

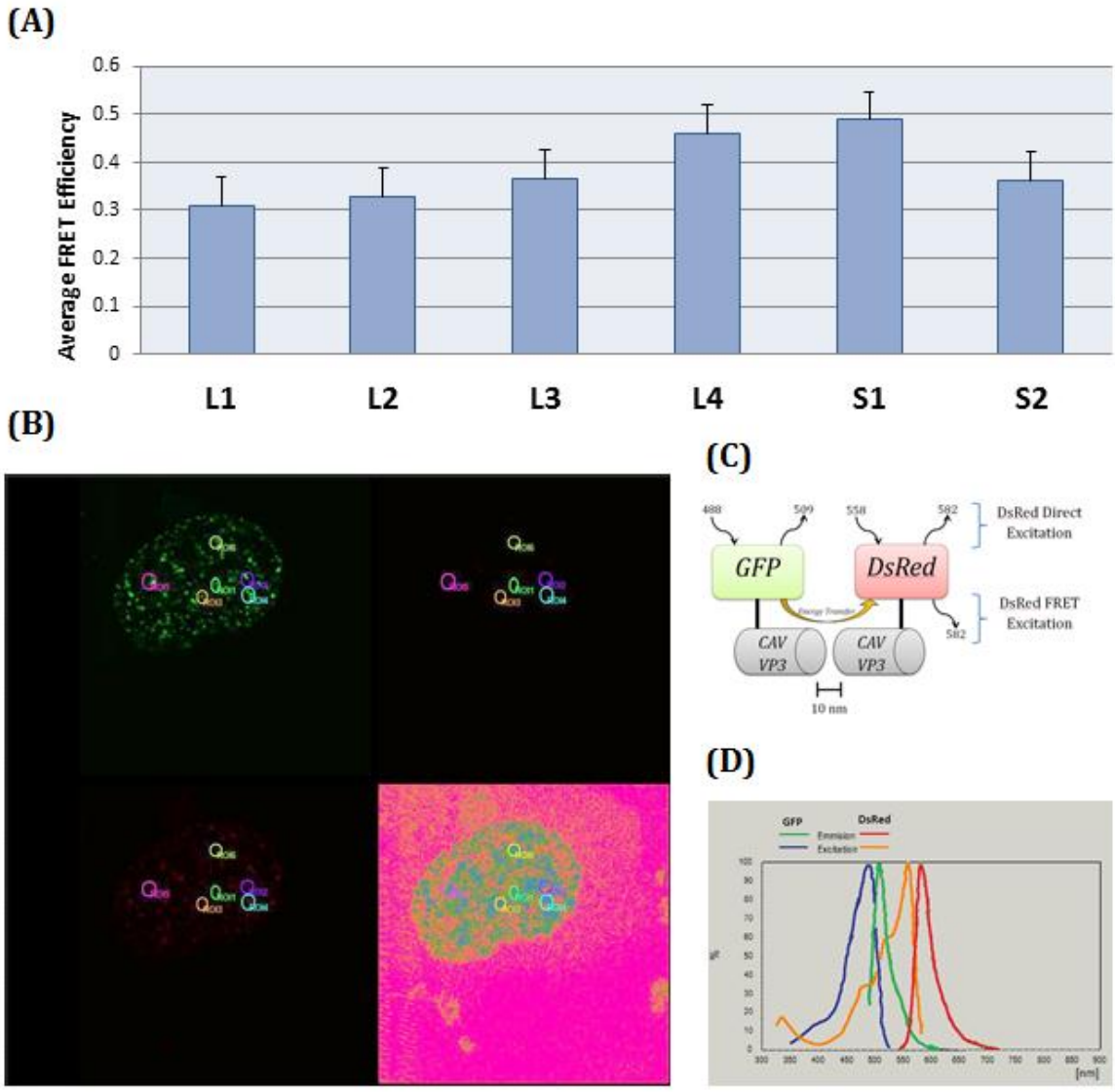

Figure 6 - GFP and DsRed-Apoptin Constructs Successfully Multimerize and initiate FRET. (A) Average FRET efficiencies were calculated for 6 different representative cells using Large (L1-L4) and Small ROIs (S1-S2) to give n = 36 for FRET values. (B) H1299 cells were transfected with GFP-Ap and DsRed-Ap and imaged under confocal microscopy. Leica FRET SE Wizard software was used to reduce background cross-talk between fluorophores and to select 6 regions of interest (ROI) in a single cell sample. Top left panel is the donor channel; top right panel is FRET channel; bottom left panel is the acceptor channel; bottom right panel is the FRET efficiency channel. This cell had an average FRET efficiency of 32.86%. (C) Schematic diagram of GFP-Ap and DsRed-Ap constructs multimerzing and undergoing FRET as GFP-Ap is excited and DsRed-Ap emitts a photon. (D) Excitation and Emission spectra of GFP and DsRed fluorophores.